Sub-proton range induced large-scale transitions in solar wind magnetic field

Tommaso Alberti, Davide Faranda, Reik V Donner, Theophile Caby, Vincenzo Carbone, Giuseppe Consolini, Berengere Dubrulle, Sandro Vaienti

Sub-proton range induced large-scale transitions in solar wind magnetic field

Tommaso Alberti*
National Institute for Astrophysics-Institute for Space Astrophysics and Planetology (INAF-IAPS), via del Fosso del Cavaliere 100, 00133, Rome, Italy

Davide Faranda
Laboratoire des Sciences du Climat et de l'Environnement, CEA Saclay l'Orme des Merisiers, UMR 8212 CEA-CNRS-UVSQ, Université Paris-Saclay & IPSL, 91191, Gif-sur-Yvette, France
London Mathematical Laboratory, 8 Margravine Gardens, London, W6 8RH, UK and
LMD/IPSL, Ecole Normale Superieure, PSL research University, 75005, Paris, France

Reik V. Donner
Department of Water, Environment, Construction and Safety, Magdeburg–Stendal University of Applied Sciences, Breitscheidstraße 2, 39114 Magdeburg, Germany and
Research Department IV – Complexity Science and Research Department I – Earth System Analysis, Potsdam Institute for Climate Impact Research (PIK) – Member of the Leibniz Association, Telegrafenberg A31, 14473 Potsdam, Germany

Theophile Caby
Université des Antilles, LAMIA, 97110 Pointe à Pitre, Guadeloupe

Vincenzo Carbone
Università della Calabria, Dipartimento di Fisica, Ponte P. Bucci, Cubo 31C, 87036, Rende (CS), Italy

Giuseppe Consolini

National Institute for Astrophysics-Institute for
Space Astrophysics and Planetology (INAF-IAPS),
via del Fosso del Cavaliere 100, I-00133, Rome, Italy

Berengere Dubrulle
SPEC, CEA, CNRS, Université Paris-Saclay,
F-91191 CEA Saclay, Gif-sur-Yvette, France

Sandro Vaienti
Aix Marseille Université, Université de Toulon, CNRS, 13009 Marseille, France

(Dated: March 22, 2021)

Abstract

We investigate the role of sub-proton dynamics in inducing large-scale transitions in the solar wind magnetic field by means of dynamical systems metrics based on instantaneous fractal dimensions. By looking at the corresponding multiscale features, we observe a break in the average attractor dimension occurring at the crossover between the inertial and the sub-proton regime. Our analysis suggests that large-scale transitions are induced by sub-proton dynamics through an inverse cascade mechanism driven by local correlations, while electron contributions (if any) are hidden by instrumental noise.

The solar wind has been shown to be a natural laboratory for plasma physics, covering a wide range of scales and being characterized by a large variety of phenomena as turbulence, intermittency, waves, instabilities, and so on [1]. A lot of attention has been directed towards understanding the scale-invariant features and self-organization of both the MHD/inertial and the kinetic/dissipative regimes [2–4]. Indeed, by searching for scaling-law behaviors and looking at high-order statistics several insights have been provided on turbulence and intermittency [5] as well as on both the direct and inverse energy/enstrophy cascade mechanisms [6, 7]. When exploring the multiscale variability of solar wind parameters, these approaches are not able to investigate scale-to-scale effects, only providing a global view of the system over a specific range of scales. Moreover, with the solar wind being characterized by nonlinearities, emergent phenomena, and cross-scale coupling, the natural framework to obtain a suitable description of scale-dependent features is via dynamical system theory [8, 9]. Within this framework, Alberti *et al.* [10] recently introduced a novel formalism to deal with the characterization of the multiscale nature of fluctuations by deriving suitable multiscale measures of complexity when looking at the behavior of scale-dependent phase-space trajectories. The basic idea is to combine a time series decomposition method (like Empirical Mode Decomposition [11]) and the concept of generalized fractal dimensions [12] to characterize how complexity varies among scales in a complex system, allowing a description of scale-dependent underlying (multi)fractal features [10]. Let $x(t)$ be a time series assumed to be composed of dynamical patterns at a "collection" of scales, i.e., $x(t) = x_0 + \sum_\tau \delta_\tau x(t)$, with $\delta_\tau x(t)$ being a fluctuation at a mean scale τ and x_0 the steady-state average value.

* tommaso.alberti@inaf.it

Then, for each scale τ' we can define a natural measure $\mu_{\tau'}$ such that

$$D_{q,\tau'} = \frac{1}{q-1} \lim_{\ell \to 0} \frac{1}{\log \ell} \log \int d\mu_{\tau'}(x) \mu_{\tau'} \left(B_{x,\tau'}(\ell) \right)^{q-1}, \tag{1}$$

with $B_{x,\tau'}(\ell)$ being the hyperball of size ℓ centered at the point x on the scale-dependent phase-space of $\sum_{\tau<\tau'} \delta_\tau x(t)$ [10]. This approach has been demonstrated to be very promising for revealing different dynamical features and behaviors of both paradigmatic model systems and real-world time series [10, 13]. A modification of this newly introduced formalism is to replace the generalized fractal dimensions, allowing a global topological and geometric view of the scale-dependent phase-space, with instantaneous measures of the actual degrees of freedom of a system, namely the local dimension [14] and phase-space local persistence. As shown by Caby *et al.* [15], these quantities can be formally related to generalized fractal dimensions and the local stability of the system. In particular, the distribution of the local dimensions is modulated by the multifractal properties of the system.

In this Letter, we extend the formalism introduced by Alberti *et al.* [10] to characterize the scale-dependent phase-space topology of solar wind magnetic field fluctuations over a wide range of scales, moving from the kinetic, through the sub-proton to the inertial scales. We use measurements coming from the Fast Plasma Investigation (FPI) instrument on board of the Magnetospheric Multiscale Mission (MMS) satellites. Our goal is to test whether this formalism is able to highlight the nature of the sudden changes in the large-scale dynamics of the solar wind by looking at the interplay between the sub-proton and the inertial range in triggering those transitions.

On November 24, 2017, the MMS orbit allowed to collect measurements in the pristine solar wind, well outside the Earth's magnetosheath and the bow shock, for a long period (i.e., a few times longer than the typical correlation scale) of approximately 1 hour from 01:10 to 02:10 UT. Figure 1 (upper panel) displays an overview of the magnetic field measurements collected by the FIELDS instrument suite [16] on board of MMS1 with a temporal resolution $\Delta t = 128$ sample/s [17].

With the solar wind being usually considered as an example for nonlinear multiscale dynamical systems, we diagnose its dynamical properties of the instantaneous (in time) and local (in phase-space) states as represented by the three components of the magnetic field. We use two dynamical systems metrics [18], the local dimension (d) and the inverse persistence (θ). The former is a measure of the active number of degrees of free-

dom, while the latter is a measure of phase-space persistence [19, 20]. Those instantaneous metrics are obtained by sampling the recurrences of a state ζ_B and observing that they are distributed according to extreme value theory. Formally, let ζ_B be a state of interest in phase-space and $g(B(t), \zeta_B) = -\log\left[\text{dist}(B(t), \zeta_B)\right]$ be the logarithmic return, where $\text{dist}(B(t), \zeta_B)$ is the Euclidean distance between $B(t)$ and ζ_B. If we define exceedances as $X(\zeta_B) = g(B(t), \zeta_B) - s(q, \zeta_B)$, with $s(q, \zeta_B)$ being an upper threshold corresponding to the q–th quantile of $g(B(t), \zeta_B)$, then the Freitas-Freitas-Todd theorem modified by Lucarini *et al.* [21] states that the cumulative distribution $F(X, \zeta_B)$ converges to the exponential member of the Generalized Pareto family

$$F(X, \zeta_B) \simeq \exp\left[-\theta(\zeta_B)\frac{X(\zeta_B)}{d^{-1}(\zeta_B)}\right], \tag{2}$$

where $0 \leq d < \infty$ is the local dimension and $0 \leq \theta \leq 1$ is the inverse persistence of the state ζ_B in units of Δt [22]. Figure 1 shows the behavior of the local dimension d (middle panel) and the inverse persistence θ (lower panel). For all computations, we fix $q = 0.98$.

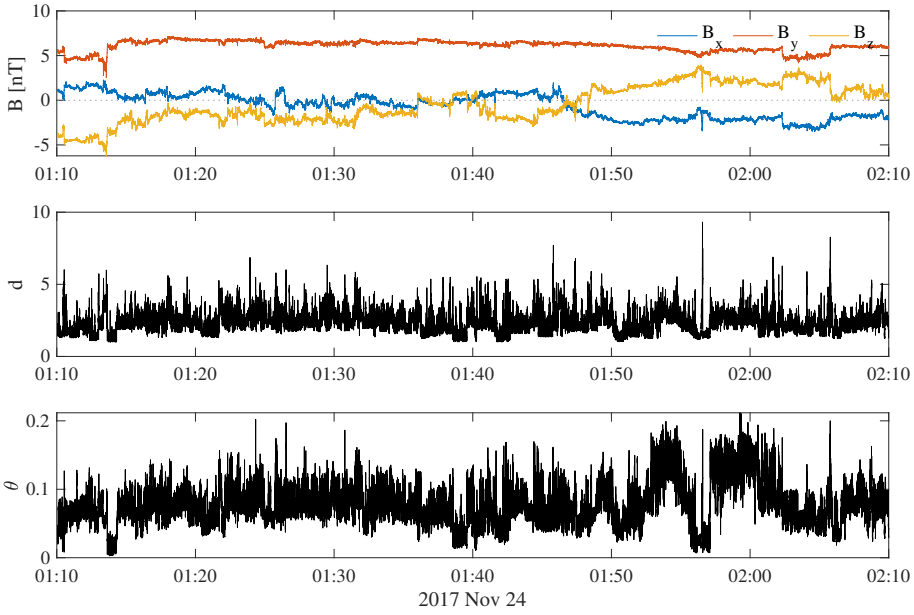

FIG. 1. (From top to bottom) The magnetic field components in the GSE reference system collected by the flux-gate magnetometer (FGM) on board of MMS1 at a resolution of $\Delta t = 128$ sample/s, the local dimension d, and the inverse persistence θ. The blue, red, and yellow lines refer to B_x, B_y, and B_z, respectively.

We observe a wide range of variability for the local dimension of $1 \lesssim d \lesssim 9$ with an average value $\langle d \rangle = 2.3 \pm 0.3$, while the inverse persistence θ is strictly confined to values

lower than 0.2 with $\langle\theta\rangle = 0.07 \pm 0.02$. This suggests that globally, the number of degrees of freedom is less than the phase-space dimension (i.e., $\langle d\rangle < 3$). This means that the dynamics is different from that of a stochastic process, for which d should exhibit small fluctuations around 3 and $\theta = 1$ [23]. A visual inspection suggests that larger d, θ are found in close correspondence with sudden changes in both B_x and B_z. The high number of degrees of freedom ($d > 3$) associated with sudden variations in magnetic field components suggests the existence of an unstable fixed point in the proximity of the transitions [14]. This is also observed in fluid turbulence showing multi-stability [24] and hints at the existence of an underlying strange stochastic attractor, i.e., the system lies in a subset of points of the whole phase-space. Indeed, although the cascade mechanism involves a wide range of scales, some of them seem to be less important than others and their description can arise from stochastic theory [24]. However, only looking at the whole time series does not provide information on the topology and the triggers of these transitions which depend on processes occurring at different scales.

To complete this analysis, we use Multivariate Empirical Mode Decomposition (MEMD) [25] to evaluate the scale-dependent fluctuations of magnetic field measurements. By defining the multivariate signal $\mathbf{B}_\mu(t) = [B_x(t), B_y(t), B_z(t)]^T$, MEMD acts on its multivariate instantaneous properties to decompose it into a finite number of multivariate oscillating patterns $\mathbf{C}_{\mu,k}(t)$, called Multivariate Intrinsic Mode Functions (MIMFs), and a monotonic trend $\mathbf{R}_\mu(t)$ as

$$\mathbf{B}_\mu(t) = \sum_{k=1}^{N} \mathbf{C}_{\mu,k}(t) + \mathbf{R}_\mu(t). \tag{3}$$

The core of the MEMD is the so-called *sifting process* that allows to derive the MIMFs in an adaptive way by exploiting the instantaneous local properties of a signal in terms of local extrema interpolation [see Ref. 25, for more details]. Each $\mathbf{C}_{\mu,k}(t)$ is a multivariate pattern representative of a peculiar dynamical feature that evolves on a typical mean scale

$$\tau_k = \frac{1}{T}\int_0^T t' \langle \mathbf{C}_{\mu,k}(t')\rangle_\mu dt', \tag{4}$$

with T being the total length of the signal and $\langle\cdots\rangle_\mu$ denoting an ensemble average over the μ-dimensional space [13]. Moreover, the spectral features of the multivariate signal $\mathbf{B}_\mu(t)$ can also be easily investigated by introducing an estimator of the power spectral density (PSD) as

$$S(\tau) = \left(\mathbb{E}\left[\mathbf{C}^2_{\mu,k}(t)\right] - \mathbb{E}\left[\mathbf{C}_{\mu,k}(t)\right]^2\right) \cdot \tau_k, \tag{5}$$

where $\mathbb{E}$ denotes the expectation value. Thus, MEMD is particularly suitable for deriving scale-dependent patterns embedded in magnetic field data, providing the starting point for a multiscale characterization of the different dynamical regimes. The multivariate signal $\mathbf{B}_\mu(t)$ is now interpreted as a collection of scale-dependent fluctuations belonging to different dynamical regimes (noise, kinetic, sub-proton, inertial, ...) that can be used to investigate how they contribute to the collective properties of the whole measurements. Indeed, following Alberti *et al.* [10], we can describe the dynamics at scales $\tau' < \tau$ as

$$\mathbf{B}_\mu^\tau(t) = \sum_{k|\tau_k<\tau} \mathbf{C}_{\mu,k}(t) \tag{6}$$

such that we can define a scale-dependent local dimension d_k and inverse persistence θ_k by diagnosing the dynamical properties of $\mathbf{B}_\mu^\tau(t)$. To do this, we compute both d_k and θ_k for reconstructions of the first k MIMFs as in Eq. (3) until $k \to N$ for which $(d_k, \theta_k) \to (d, \theta)$. Figure 2 shows the distributions of both the local dimension and the inverse persistence as a function of the different scales τ.

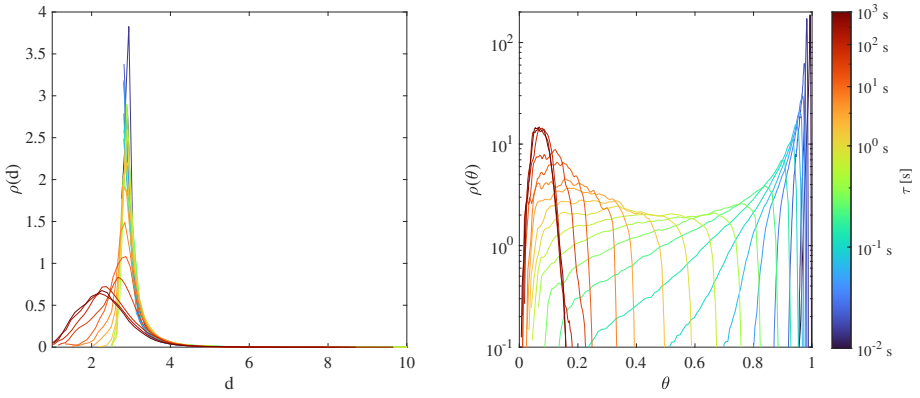

FIG. 2. Probability distribution functions $\rho(\cdot)$ of the local dimension d (left panel) and the inverse persistence θ as a function of the scale τ (colored lines).

We observe a decreasing d and a decreasing θ as τ increases, suggesting that the whole phase-space properties resemble those of a low-dimensional dynamical system. This is again reminiscent of the fluid-dynamical behavior as observed in the turbulent von Karman swirling flow, which despite very high Reynolds number, has been characterized by a low-dimensional stochastic attractor [24]. Conversely, larger d and larger θ characterize the short-term variability of the solar wind magnetic field, providing evidence for an underlying higher-dimensional structure. This seems to suggest a dynamical transition in the underly-

ing structure of the phase-space when moving from short- to long-term dynamics, i.e., when passing from sub-proton to inertial scales. To better underline these features we evaluate the average values of d and θ at the different scales τ and compared with the behavior of the PSD $S(\tau)$ (see Eq. 5) as reported in Figure 3.

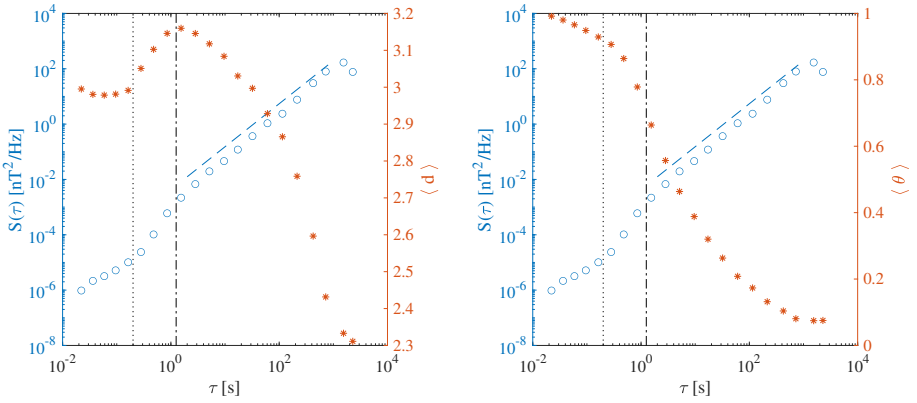

FIG. 3. Average values $\langle d \rangle$ (left panel, red asterisks) and $\langle \theta \rangle$ (right panel, red asterisks) at the different scales τ as compared with the behavior of the PSD $S(\tau)$ (blue circles). The dashed and dashed-dotted lines indicate the FGM instrumental noise limit ($f \sim 5$ Hz) to the inverse of the proton-cyclotron frequency ($f_{c_p} = 1/\tau_{c_p} = eB/m_p$), respectively. The dashed blue line highlights the Kolmogorov-like spectral scaling $\sim \tau^{5/3}$.

The behavior of $S(\tau)$ evidences the existence of three different dynamical regimes: the instrumental noise range for $\tau < 0.2$ s, the sub-proton range for 0.2 s $< \tau <$ 1.3 s, and the inertial range for $\tau > 1.3$ s. These findings are well in agreement with the results of Bandyopadhyay *et al.* [17]. By looking at the behavior of $\langle d \rangle$ and $\langle \theta \rangle$ at the different scales τ we clearly observe a scale-dependent behavior of $\langle d \rangle$ that resembles that highlighted by $S(\tau)$. The instrumental noise regime is characterized by $\langle d \rangle = 3$ and $\langle \theta \rangle \approx 1$ suggesting, as expected, a purely stochastic origin for the short-term variability of magnetic field fluctuations (i.e., $\tau < 0.2$ s). From a dynamical system point of view, this means that ergodicity characterizes the phase-space, i.e., there exists a reference trajectory of a "typical" point that can be used for deducing the average behavior of the system.

The sub-proton regime ($\tau_{noise} < \tau < \tau_{c_p}$) is instead characterized by an increasing $\langle d \rangle$ as τ increases, reaching a maximum value $\langle d \rangle_{max} \approx 3.2$ for $\tau \sim \tau_{c_p}$ (i.e., larger than the topological dimension of the system), together with a nonlinear decreasing $\langle \theta \rangle$ with τ, reaching an inflection point for $\tau \sim \tau_{c_p}$. These features have not been reported before in the literature

and can be interpreted as an increase in the average number of degrees of freedom at sub-proton scales due to the nonlinear energy cascade effects moving energy towards these scales [5]. Moreover, the behavior of $\langle d \rangle$ and $\langle \theta \rangle$ at $\tau \sim \tau_{c_p}$ is clearly the reflection of a dynamical transition occurring at the boundary between the sub-proton and the inertial regimes. Indeed, going towards larger scales (i.e., approaching the inertial range), we observe a decreasing $\langle d \rangle$ and $\langle \theta \rangle$ with τ, reflecting a reduced-order nature of large-scale magnetic field fluctuations with an active number of degree of freedom that is lower than the topological dimension of the system ($\langle d \rangle < 3$). This points towards the possibility to describe the dynamics across the inertial range as a low-dimensional dynamical system [9]. Furthermore, the reduced values of $\langle \theta \rangle$ suggest a long residence time of the system in the dynamical states corresponding to the inertial range, indicating that they can be interpreted as a collection of marginally stable fixed points of the dynamics with sub-proton scale induced transitions. Taking together the above results, we can firmly state that (i) the inertial range dynamics can be easily described as a reduced-order dynamical system, and (ii) the increasing dimensionality of the sub-proton regime is a reflection of small-scale turbulence-induced magnetic field fluctuations due to a dynamical component that is external to the sub-proton physics, i.e., dynamical information is introduced from processes occurring through the inertial regime and reflecting a direct energy cascade mechanism.

To further support the claim that a larger number of degrees of freedom in magnetic field fluctuations is only due to processes occurring at sub-proton scales while global properties are mainly related to inertial processes, we compare the behavior of the $d - \theta$ plane at two different scales τ_{c_p} and τ_I, with τ_I being the largest scale belonging to the inertial range (i.e., $\tau_I \sim 10^3$ s) in dependence on the ratio between magnetic field fluctuations at that scale and their standard deviation as reported in Fig. 4.

We observe that larger values of d are associated with larger fluctuations at sub-proton scales, thus suggesting a key role of the organization of sub-proton scales in regulating the active number of degrees of freedom of the system. We also show that a very wide range of θ values is observed at sub-proton scales, thus reflecting an unstable (from a dynamical system point of view) nature of fluctuations within this regime. Conversely, when inertial scales are reached we evidence a reduced range of θ, confined below 0.2, together with a clearly narrower range of d with respect to the sub-proton regime. This suggests that the MHD dynamics is dominated by marginally stable fixed points conferring a low-dimensional

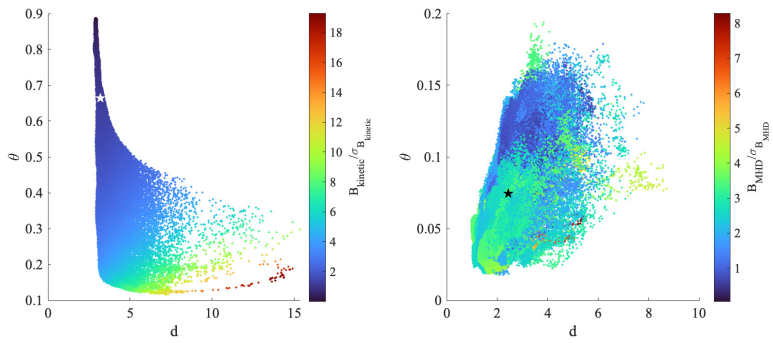

FIG. 4. $d - \theta$ plane at two different scales τ_{c_p} (left) and τ_I (right) in dependence on the ratio between magnetic field fluctuations at that scale and their standard deviation (colors). White and black asterisks correspond to the mean values of d and θ at the two different scales.

nature to the system.

To quantitatively demonstrate these observations, we evaluated the mutual information [26] between d (θ) and $\mathbf{B}_\mu^\tau(t)$ (Eq. 6) as shown in Fig. 5. A statistically significant dependency is clearly found between d and magnetic field fluctuations below the proton-cyclotron scale τ_{c_p} as well as between θ and the inertial range dynamics ($\tau \gtrsim \tau_{c_p}$). This quantitatively shows that the overall dynamics of solar wind magnetic field variability reflects those observed at inertial scales, being characterized by a low-dimensional dynamics around marginally stable fixed points, while a larger number of degrees of freedom in conjunction with an unstable nature of the phase-space topology reflecting an externally forced dynamics is associated with the sub-proton range dynamics. The kinetic and electron scales contributions (if any) to the dynamics remain difficult to evaluate because of the prominent role of the noise overriding the kinetic and electron scales contributions at high frequency.

Our results provide the first quantitative evidence of large-scale turbulence-induced fluctuations, thus being a quantitative proof of the Richardson cascade effects on the sub-proton regime from the inertial one. We found that the number of degrees of freedom is larger than the topological dimension of the system as represented by the magnetic field ($D = 3$) at sub-proton scales ($\tau > \tau_{c_p}$), while a low-dimensional phase-space is found at MHD scales ($\tau < \tau_{c_p}$). On one hand, this suggests the existence of an externally induced dynamics at sub-proton scales that can be related to the inertial range direct cascade mechanism; on the other hand, this also implies that there exists a degree of correlation between magnetic field components that tends to reduce the effective number of degrees of freedom at

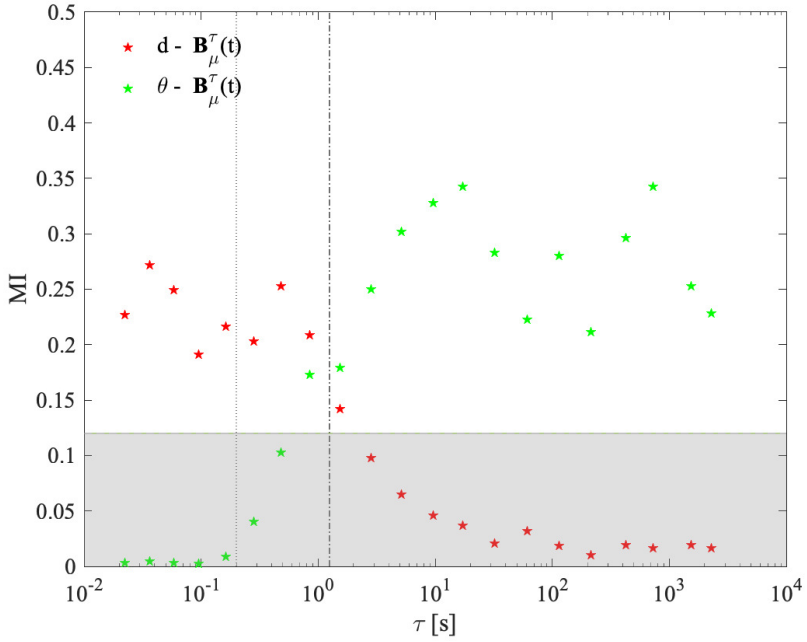

FIG. 5. Mutual information between d and $\mathbf{B}_\mu^\tau(t)$ (red) and between θ and $\mathbf{B}_\mu^\tau(t)$ (green). The dashed and dashed-dotted lines correspond to the FGM instrumental noise cutoff ($f \sim 5$ Hz) and the inverse of the proton-cyclotron frequency ($f_{c_p} = 1/\tau_{c_p} = eB/m_p$), respectively. The gray shaded area denotes the 95% significance level.

MHD scales. The latter result points towards a 2D nature of magnetic field fluctuations at MHD scales with an inverse enstrophy cascade typically arising in near two-dimensional incompressible decaying turbulence. Taken together, we firmly demonstrated that sudden variations observed in magnetic field measurements are associated with unstable fixed points characterizing the dynamics at sub-proton scales. These large-scale intermittent-like variations cannot be definitely associated with coherent intermittent events belonging to the MHD domain, but seem to be related to an underlying stochastic strange attractor [27], in close analogy with the results obtained by Raphaldini *et al.* [28, 29] for MHD and Faranda *et al.* [24] for fluid turbulence. Indeed, we also demonstrated the existence of a different fixed point nature across the different scales, moving from an unstable point approached at sub-proton scales to marginally stable fixed points at inertial scales. Thus, the overall dynamics of solar wind magnetic field fluctuations consists of multi-stable and multiscale fixed points, opening a novel way to describe the solar wind via stochastic low-dimensional models featuring a large number of degrees of freedom [24, 27].

ACKNOWLEDGMENTS

We acknowledge the MMS team and instrument leads for data access and support. The data presented in this paper are the L2 data of MMS and can be accessed from the MMS Science Data Center (https://lasp.colorado.edu/mms/sdc/public/). TA, RVD, and GC acknowledge fruitful discussions within the scope of the International Team "Complex Systems Perspectives Pertaining to the Research of the Near-Earth Electromagnetic Environment" at the International Space Science Institute in Bern, Switzerland.

---

[1] R. Bruno and V. Carbone, *Turbulence in the Solar Wind*, Vol. 928 (2016).

[2] V. Carbone, Scalings, Cascade and Intermittency in Solar Wind Turbulence, Space Sci. Rev. **172**, 343 (2012).

[3] W. H. Matthaeus, M. Wan, S. Servidio, A. Greco, K. T. Osman, S. Oughton, and P. Dmitruk, Intermittency, nonlinear dynamics and dissipation in the solar wind and astrophysical plasmas, Philosophical Transactions of the Royal Society of London Series A **373**, 20140154 (2015).

[4] D. Verscharen, K. G. Klein, and B. A. Maruca, The multi-scale nature of the solar wind, Living Reviews in Solar Physics **16**, 5 (2019), arXiv:1902.03448 [physics.space-ph].

[5] A. N. Kolmogorov, Dissipation of Energy in Locally Isotropic Turbulence, Akademiia Nauk SSSR Doklady **32**, 16 (1941).

[6] W. H. Matthaeus and M. L. Goldstein, Measurement of the rugged invariants of magnetohydrodynamic turbulence in the solar wind, J. Geophys. Res. **87**, 6011 (1982).

[7] L. Sorriso-Valvo, R. Marino, V. Carbone, A. Noullez, F. Lepreti, P. Veltri, R. Bruno, B. Bavassano, and E. Pietropaolo, Observation of Inertial Energy Cascade in Interplanetary Space Plasma, Phys. Rev. Lett. **99**, 115001 (2007), arXiv:astro-ph/0702264 [astro-ph].

[8] V. Carbone and P. Veltri, Relaxation processes in magnetohydrodynamics - A triad-interaction model, Astron. Astrophys. **259**, 359 (1992).

[9] T. Alberti, G. Consolini, and V. Carbone, A discrete dynamical system: The poor man's magnetohydrodynamic (PMMHD) equations, Chaos **29**, 103107 (2019).

[10] T. Alberti, G. Consolini, P. D. Ditlevsen, R. V. Donner, and V. Quattrociocchi, Multiscale measures of phase-space trajectories, Chaos **30**, 123116 (2020).

[11] N. E. Huang, Z. Shen, S. R. Long, M. C. Wu, H. H. Shih, Q. Zheng, N. C. Yen, C. C. Tung, and H. H. Liu, The empirical mode decomposition and the Hilbert spectrum for nonlinear and non-stationary time series analysis, Proceedings of the Royal Society of London Series A **454**, 903 (1998).

[12] H. G. E. Hentschel and I. Procaccia, The infinite number of generalized dimensions of fractals and strange attractors, Physica D Nonlinear Phenomena **8**, 435 (1983).

[13] T. Alberti, R. V. Donner, and S. Vannitsem, Multiscale fractal dimension analysis of a reduced order model of coupled ocean-atmosphere dynamics, Earth System Dynamics Discussions **2021**, 1 (2021).

[14] D. Faranda, V. Lucarini, G. Turchetti, and S. Vaienti, Generalized Extreme Value Distribution Parameters as Dynamical Indicators of Stability, International Journal of Bifurcation and Chaos **22**, 1250276 (2012), arXiv:1107.5972 [math.DS].

[15] T. Caby, D. Faranda, G. Mantica, S. Vaienti, and P. Yiou, Generalized dimensions, large deviations and the distribution of rare events, Physica D Nonlinear Phenomena **400**, 132143 (2019), arXiv:1812.00036 [math.DS].

[16] R. B. Torbert, C. T. Russell, W. Magnes, R. E. Ergun, P. A. Lindqvist, O. Le Contel, H. Vaith, J. Macri, S. Myers, D. Rau, J. Needell, B. King, M. Granoff, M. Chutter, I. Dors, G. Olsson, Y. V. Khotyaintsev, A. Eriksson, C. A. Kletzing, S. Bounds, B. Anderson, W. Baumjohann, M. Steller, K. Bromund, G. Le, R. Nakamura, R. J. Strangeway, H. K. Leinweber, S. Tucker, J. Westfall, D. Fischer, F. Plaschke, J. Porter, and K. Lappalainen, The FIELDS Instrument Suite on MMS: Scientific Objectives, Measurements, and Data Products, Space Sci. Rev. **199**, 105 (2016).

[17] R. Bandyopadhyay, A. Chasapis, R. Chhiber, T. N. Parashar, B. A. Maruca, W. H. Matthaeus, S. J. Schwartz, S. Eriksson, O. Le Contel, H. Breuillard, J. L. Burch, T. E. Moore, C. J. Pollock, B. L. Giles, W. R. Paterson, J. Dorelli, D. J. Gershman, R. B. Torbert, C. T. Russell, and R. J. Strangeway, Solar Wind Turbulence Studies Using MMS Fast Plasma Investigation Data, The Astrophys. J. **866**, 81 (2018), arXiv:1807.06140 [physics.space-ph].

[18] V. Lucarini, D. Faranda, and J. Wouters, Universal Behaviour of Extreme Value Statistics for Selected Observables of Dynamical Systems, Journal of Statistical Physics **147**, 63 (2012), arXiv:1110.0176 [cond-mat.stat-mech].

[19] N. R. Moloney, D. Faranda, and Y. Sato, An overview of the extremal index, Chaos **29**, 022101

(2019).

[20] T. Caby, D. Faranda, S. Vaienti, and P. Yiou, On the Computation of the Extremal Index for Time Series, Journal of Statistical Physics **179**, 1666 (2019), arXiv:1904.04936 [math.DS].

[21] V. Lucarini, D. Faranda, J. Wouters, and T. Kuna, Towards a General Theory of Extremes for Observables of Chaotic Dynamical Systems, Journal of Statistical Physics **154**, 723 (2014), arXiv:1301.0733 [cond-mat.stat-mech].

[22] A. C. Moreira Freitas, J. Milhazes Freitas, and M. Todd, Extremal Index, Hitting Time Statistics and periodicity, arXiv e-prints , arXiv:1008.1350 (2010), arXiv:1008.1350 [math.PR].

[23] D. Faranda, J. Milhazes Freitas, V. Lucarini, G. Turchetti, and S. Vaienti, Extreme value statistics for dynamical systems with noise, Nonlinearity **26**, 2597 (2013), arXiv:1208.5582 [math.DS].

[24] D. Faranda, Y. Sato, B. Saint-Michel, C. Wiertel, V. Padilla, B. Dubrulle, and F. Daviaud, Stochastic Chaos in a Turbulent Swirling Flow, Phys. Rev. Lett. **119**, 014502 (2017), arXiv:1607.08409 [physics.flu-dyn].

[25] N. Rehman and D. P. Mandic, Multivariate empirical mode decomposition, Proceedings of the Royal Society of London Series A **466**, 1291 (2010).

[26] Given two signals $s_1(t)$ and $s_2(t)$ the mutual information is defined as MI= $\sum_{j,k} p(s_1(t_j), s_2(t_k)) \log \frac{p(s_1(t_j), s_2(t_k))}{p(s_1(t_j))p(s_2(t_k))}$ where $p(s_1, s_2)$ is the joint probability of observing the pair of values (s_1, s_2), while $p(s_1)$ and $p(s_2)$ are the independent distributions. For statistically independent time series MI= 0, while for correlated time series MI $\geq$MI$_{th}$, a threshold associated with a particular statistical significance level (e.g., 95%).

[27] V. Carbone, F. Lepreti, A. Vecchio, T. Alberti, and F. Chiappetta, On the origin of high-frequency magnetic fluctuations in the interplanetary medium: a Brownian-like approach , Frontiers in Physics **in press**, 10.3389/fphy.2021.613759 (2021).

[28] B. Raphaldini, D. Ciro, E. S. Medeiros, L. Massaroppe, and R. I. F. Trindade, Evidence for crisis-induced intermittency during geomagnetic superchron transitions, Phys. Rev. E **101**, 022206 (2020), arXiv:1905.05834 [physics.geo-ph].

[29] B. Raphaldini, E. S. Medeiros, D. Ciro, D. R. Franco, and R. I. F. Trindade, Geomagnetic reversals at the edge of regularity, Physical Review Research **3**, 013158 (2021), arXiv:2006.15420 [physics.geo-ph].